IEEE TRANSACTIONS ON MICROWAVE THEORY AND TECHNIQUES, VOL. MTT-21, NO. 11, NOVEMBER 1973

Nonlinear and Large-Signal Characteristics of Millimeter-Wave IMPATT Amplifiers

H. J. KUNO AND DAVID L. ENGLISH

Abstract—**Experimental results obtained with millimeter-wave IMPATT amplifiers are presented. Nonlinear and large-signal characteristics of stable IMPATT amplifiers and injection-locked IMPATT oscillators are described. Amplifier circuit configuration, diode characteristics, and measured effects of bias current, temperature, and large-signal level on gain, bandwidth, power saturation, and phase-delay characteristics are discussed in detail.**

INTRODUCTION

IT has been shown that IMPATT diodes can be used for amplification of millimeter-wave signals as well as for generation of millimeter-wave power [1]–[5]. Recently, applications of IMPATT diodes in millimeter-wave communication systems have increasingly become of great interest and importance. In particular, it has been demonstrated that IMPATT amplifiers can be used effectively for amplification of millimeter-wave phase-modulated signals in high data-rate communication systems [1]–[3]. This paper presents experimental results obtained with millimeter-wave Si IMPATT amplifiers developed for such applications. Amplification of phase-modulated signals may be accomplished with an IMPATT diode operated either as a stable amplifier or an injection-locked oscillator. Described in this paper are an amplifier circuit configuration, IMPATT-diode characteristics, nonlinear gain–bandwidth characteristics, large-signal effects on gain–bandwidth and phase-delay characteristics, and bias current and temperature effects on gain and power saturation characteristics.

IMPATT-DIODE CHARACTERISTICS

IMPATT amplifier performance is strongly related to dc characteristics of the IMPATT diode, which is in turn related to the doping density profile and function geometry. Shown in Fig. 1 is the doping density profile of an IMPATT diode designed for 60-GHz operation. It consists of a thin layer of diffused (or ion-implanted) heavily doped p^+-type region, an epitaxially grown n-type region, and a low-resistivity n^+-type substrate. Critical material parameters that determine RF performance of the diode are the doping density and the thickness of the n-type epitaxial layer, the p^+-n junction and n-n^+ interface. The doping density transition at the n-n^+ interface should be made as abrupt as possible. If this interface is excessively graded, a high parasitic series resistance results that reduces the output power and efficiency. The p^+-n junction should also be made abrupt. The graded junction results in reduced output power and efficiency. The n-type region should be doped uniformly. The graded doping density profile reduces the output power capability of the diode. The doping density and thickness of the n-type region should be made

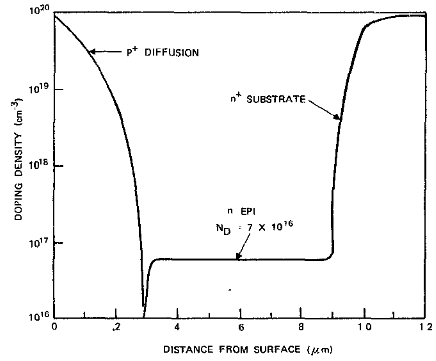

Fig. 1. Doping density profile design of a 60-GHz IMPATT diode.

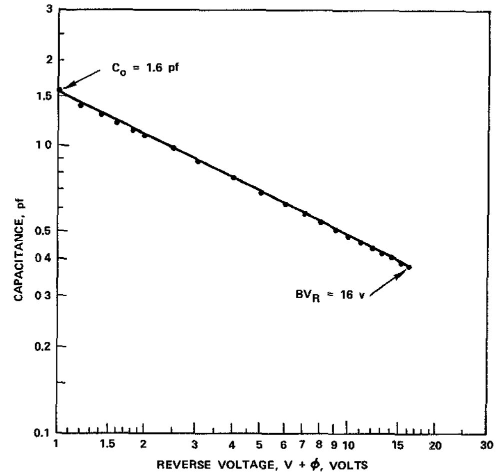

Fig. 2. *C–V* characteristics of a 60-GHz IMPATT diode.

such that, at the operational bias current level and the operational junction temperature, the space-charge region critically punches through, i.e., the edge of the space-charge region reaches the n^+ region at the operational bias current level. If the n-type region is under critically doped, excessive punch through occurs. If it is over critically doped, an unswept region remains at the n-n^+ interface that increases a series resistance. In either case, the out-power capability of the diode will be lower than that of the critically doped diode. The space-charge region width is related to the transit time of the drifting electrons. The optimum transit angle is approximately 0.75π [6], [7]. In the doping density profile design of the 60-GHz IMPATT diode shown in Fig. 1, we use the value of 0.8×10^7 cm/s as the saturated electron drift velocity at the junction temperature of 200°C [10], [11]. In the design the space-charge region widening effect due to both temperature and bias current [9] has also been taken into consideration.

Shown in Fig. 2 is the capacitance variation of a typical

Manuscript received January 24, 1973; revised April 6, 1973. This work was supported in part by the Air Force Avionics Laboratory, Air Force Systems Command, U. S. Air Force, Wright-Patterson AFB, Ohio.
The authors are with the Hughes Research Laboratories, Torrance, Calif. 90509.

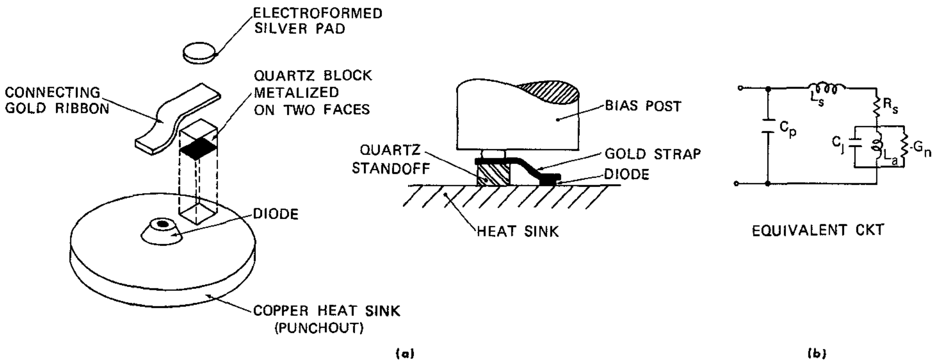

Fig. 3. (a) IMPATT-diode mounting configuration. (b) An equivalent circuit.

IMPATT diode measured as a function of bias voltage. The $C-V$ characteristics with 1/2 slope in the log–log scale indicate the abrupt junction with uniform doping density profile [8]. Fig. 3(a) shows the diode mounting configuration used for the experiment. The diode is mounted on a gold-plated OFHC copper heat sink with the junction side (p^+-region) close to the heat sink. The substrate is thinned down to 10-μm thickness. The electrical contact is made by means of a gold strap connected between the diode and a small quartz standoff block. This diode mounting technique provides very small parasitic inductance and package capacitance that reduce the gain–bandwidth capabilities of the diodes used as amplifiers, particularly at millimeter-wave frequencies.

Amplifier Circuit

Microwave characteristics of an IMPATT diode can be represented by an equivalent circuit consisting of a frequency-dependent nonlinear negative conductance $-G_n$, an avalanche inductance L_a, junction capacitance C_j, a series resistance R_s, an inductance L_s, and a capacitance C_p associated with the package and the mount as shown in Fig. 3(b). Techniques we have developed for characterizing IMPATT diodes at millimeter-wave frequencies are discussed in [12] and [13]. Both the negative conductance $-G_n$ and the avalanche inductance L_a are nonlinear parameters. They are dependent on frequency, bias current, and RF signal level.

In order to achieve optimum performance from a given device at a specific frequency, both the real and imaginary components of the circuit impedance must be matched to those of the device impedance.

It should be pointed out that in general a properly designed IMPATT circuit can be used either as an oscillator or as an amplifier by adjusting turning conditions. Shown in Fig. 4(a) is a cross-sectional view of a V-band IMPATT oscillator /amplifier circuit used in the experiment. It consists of a reduced-height waveguide cavity, an adjustable coaxial section, a movable short, and a quarter-wave impedance transformer. The reduced-height waveguide section is to reduce the effective-load impedance level so that a better match to the low impedance of the IMPATT diode can be achieved. The microwave characteristics of the amplifier circuit can be represented by an equivalent circuit shown in Fig. 4(b). The circuit possesses the unique feature of providing two degrees of tuning freedom by means of the series and parallel tuning elements provided by the adjustable coaxial section and the movable short, respectively. In this way, a broad range of loading conditions can be provided by relatively simple means.

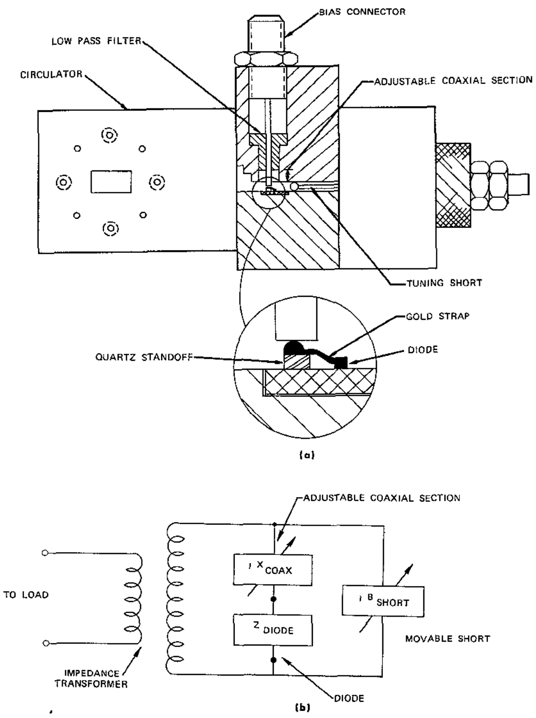

Fig. 4. (a) Cross-sectional view of a millimeter-wave IMPATT amplifier/oscillator. (b) Simplified equivalent circuit.

Experimentally loaded Q values ranging from 5 for broadband amplification to greater than 300 for low-noise oscillation have been obtained by adjusting the tuning elements.

In addition to the electrical characteristics of the circuit, it is also important to provide a good thermal path to remove heat generated in the diode. Shown in Fig. 4(a) is a detailed view of the diode mounting scheme. The diode TC bonded onto an OFHC copper heat-sink disk is mounted with tin–gold solder on a larger heat sink which is part of the circuit. Thermal resistance measured between the diode junction and the outside surface of the amplifier circuit ranges between 35 and 45° C/W for diodes operated at 60 GHz, depending on the junction area.

Stable IMPATT Amplifiers

Many stable IMPATT amplifiers have been evaluated. Fig. 5 shows the measured output versus input power transfer characteristics of an IMPATT diode operated as a stable ampli-

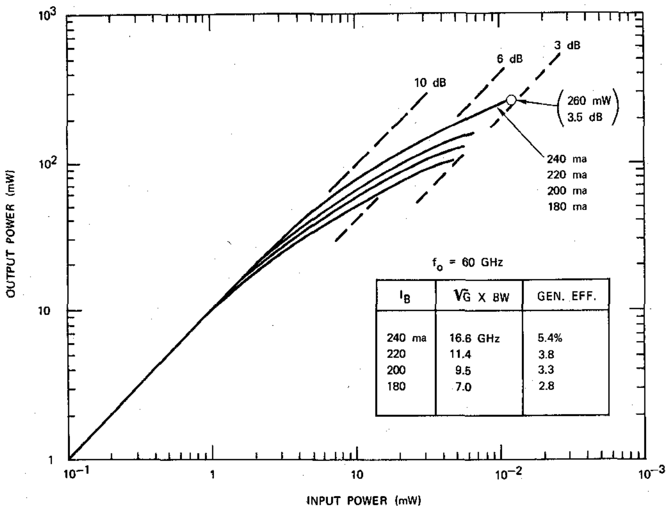

Fig. 5. Effects of bias current on power, gain–bandwidth product, and generation efficiency for a stable IMPATT amplifier.

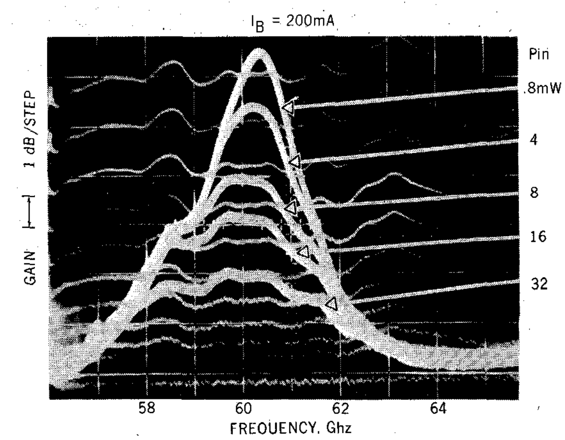

Fig. 6. Large-signal effects on gain–bandwidth characteristics of a stable IMPATT amplifier.

fier measured at various bias current levels. Also shown is the maximum power generation efficiency measured at each current level. At each current level, the amplifier was tuned for 10-dB small-signal gain. Saturated output power level, gain–bandwidth product, and the generation efficiency increased with the increasing bias current. Maximum output power of 260 mW and maximum gain–bandwidth product of 16.6 GHz and generation efficiency, $(P_{out}—P_{in})/P_{dc}$, of 5.4 percent have been obtained. This was the best gain–bandwidth product we have measured. Temperature effects on the amplifier were also measured. Over the temperature change from 23 to 65°C, the small-signal gain decreased by 0.05 dB/°C, but the saturated output power changed by only 0.01 dB/°C.

Fig. 6 shows variations of gain–bandwidth characteristics of an IMPATT amplifier measured at various input power levels. It can be seen that as the power level increases, bandwidth increases but the gain decreases. It can also be seen that the center frequency shifts to the lower side gradually with the increasing input power. As the gain and bandwidth change at large-signal levels, phase delay also changes. Shown in Fig. 7 are the changes in gain and phase delay measured as a function of input power level at the center frequency f_0 and both sides of the center frequency. As the input signal increases the phase delay increases at all frequencies. The change in phase delay as a function of the input power level results in AM–PM conversion.

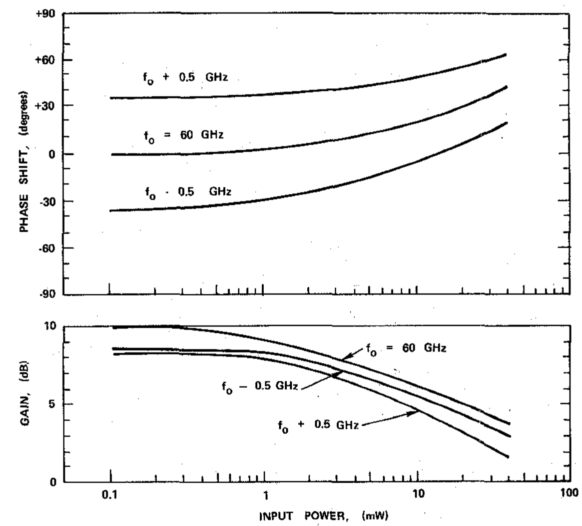

Fig. 7. Large-signal effects on gain and phase delay characteristics of a stable IMPATT amplifier.

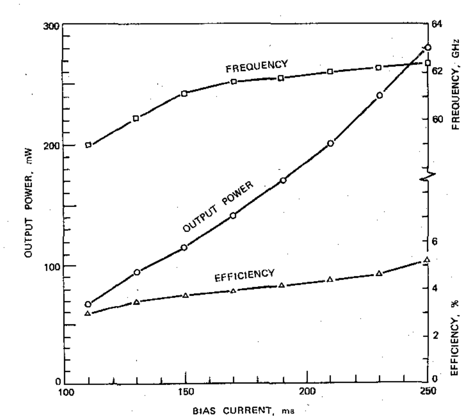

Fig. 8. Effect of bias current on power and efficiency of a free-running IMPATT oscillator.

Injection-Locked IMPATT Oscillators

Amplification of phase-modulated signals can be accomplished also with an injection-locked IMPATT oscillator. Fig. 8 shows effects of bias current on output power, efficiency, and frequency of free-running oscillation of an IMPATT diode tuned for maximum output power at each current level. Both output power and efficiency increase with the increasing bias current. The frequency of oscillation may increase or decrease with the increasing bias current depending on the tuning conditions. We found that for diodes from the same production lot higher conversion efficiencies can be obtained from diodes with smaller junction area but output power does not vary significantly with the junction size. Effects of temperature on the output power and frequency of the free-running IMPATT oscillation have also been measured. The frequency decreased with the increasing temperature at a rate of 2.75 MHz/°C in the 60-GHz range. The output power decreased with the increasing case temperature at a rate less than 0.004 dB/°C. No special effort was made to minimize the temperature effects.

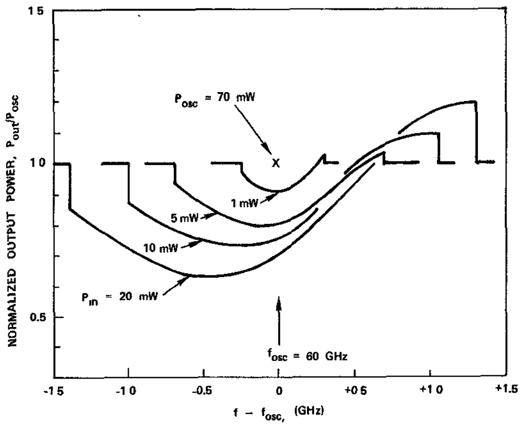

Fig. 9. Large-signal effects on locking characteristics of an injection-locked IMPATT oscillator.

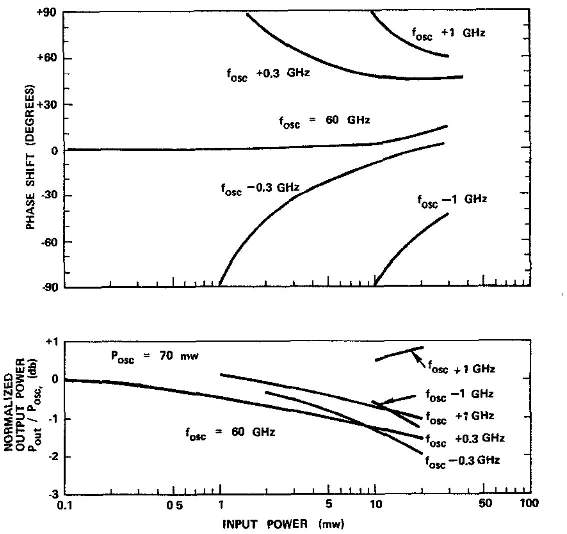

Fig. 10. Large-signal effects on output power and phase delay of an injection-locked IMPATT oscillator.

The locking gain–bandwidth characteristics of an IMPATT-diode injection-locked oscillator generally follow classical phase-locking characteristics given by

$$(P_{out}/P_{in})^{1/2}\Delta f = \text{const}$$

where Δf is the locking bandwidth and P_{out}/P_{in} is the locking power gain. Large-signal effects on locking bandwidth, output power, and phase delay are shown in Figs. 9 and 10. The locking characteristics are not symmetrical about the free-running oscillation frequency.

Conclusions

Various nonlinear and large-signal characteristics of IMPATT diodes operated as stable amplifiers and injection-locked oscillators developed for amplification of phase-modulated millimeter-wave signals have been described. Comparison of the various experimentally observed nonlinear and large-signal phenomena described in this paper with the results of the analysis [17] shows an excellent agreement. Both stable IMPATT amplifiers and injection-locked IMPATT oscillators have been used successfully for amplification of phase-modulated signals at a data rate of 1 Gbit/s [1]. It is interesting to compare characteristics of stable IMPATT amplifiers and those of injection-locked oscillators. For a given IMPATT diode, high output power with a high gain (>20 dB) but with a narrow bandwidth can be achieved from an injection-locked oscillator, while high output power with a relatively low gain (<10 dB) but with a broad bandwidth can be achieved from a stable amplifier. A stable amplifier also yields a higher gain–bandwidth product than an injection-locked oscillator. Although an injection-locked oscillator provides the suppression of amplitude modulation at the output, the AM–PM conversion will be larger in comparison with stable amplifiers.

By making use of double-drift IMPATT diodes [14]–[16] that are capable of high output power and power combination techniques [5], output power levels of more than 1 W may be feasible from an IMPATT amplifier in the millimeter-wave frequency range.

Acknowledgment

The authors wish to thank Dr. N. B. Kramer for his encouragement and support and R. Mahuex for his laboratory assistance. They also wish to thank R. S. Ying for the development of IMPATT diodes used for the experiments.

References

[1] H. J. Kuno, D. L. English, and P. H. Pusateri, "Millimeter-wave solid-state exciter/modulator-amplifier module for gigabit data-rate," presented at the IEEE Int. Microwave Symp., Chicago, Ill., May 1972.

[2] H. J. Kuno, L. S. Bowman, and F. L. English, "Millimeter-wave silicon IMPATT power amplifiers for phase-modulated signals," presented at the IEEE Int. Solid-State Circuits Conf., Philadelphia, Pa., Feb. 1971.

[3] Y. Fukatsu, M. Akaike, and H. Kato, "Amplification of high speed PCM phase-shift keyed millimeter-wave signals through an injection-locked IMPATT oscillator," presented at the IEEE Int. Solid-State Circuits Conf., Philadelphia, Pa., Feb. 1971.

[4] H. C. Bowers and L. W. Harbaugh, "High power solid-state millimeter-wave amplifiers," presented at the IEEE Int. Solid-State Circuits Conf., Philadelphia, Pa., Feb. 1973.

[5] H. J. Kuno, D. L. English, and R. S. Ying, "High power millimeter-wave IMPATT amplifiers," presented at the IEEE Int. Solid-State Circuits Conf., Philadelphia, Pa., Feb. 1973.

[6] K. Mouthaan, "Nonlinear analysis of the avalanche transit-time oscillator," *IEEE Trans. Electron Devices*, vol. 16, pp. 935–945, Nov. 1969.

[7] D. Delagebeaudeuf, "Experimental verification of approximate large-signal theory of IMPATT diodes," *Proc. IEEE* (Lett.), vol. 58, pp. 1140–1141, July 1970.

[8] J. L. Moll, *Physics of Semiconductors.* New York: McGraw-Hill, 1964.

[9] S. M. Sze, *Physics of Semiconductor Devices.* New York: Wiley-Interscience, 1969.

[10] C. Y. Duh and J. L. Moll, "Electron drift velocity in avalanching silicon diodes," *IEEE Trans. Electron Devices*, vol. ED-14, pp. 46–49, Jan. 1967.

[11] J. F. Gibbons, "Papers on carrier drift velocities in silicon at high electric field strengths—Introduction," *IEEE Trans. Electron Devices*, vol. ED-14, p. 37, Jan. 1967.

[12] H. J. Kuno, T. T. Fong, and D. L. English, "Characterization of IMPATT diodes at millimeter-wave frequencies," *IEEE Trans. Electron Devices*, vol. ED-19, pp. 752–757, June 1972.

[13] ——, "Computer-aided characterization of millimeter-wave semiconductor devices," presented at the IEEE Int. Microwave Symp., Washington, D.C., May 1971.

[14] D. L. Scharfetter, W. J. Evans, and R. L. Johnston, "Double-drift-region (p^+pnn^+) avalanche diode oscillators," *Proc. IEEE* (Lett.), vol. 58, pp. 1131–1133, July 1970.

[15] T. E. Seidel and D. L. Scharfetter, "High-power millimeter wave IMPATT oscillators with both hole and electron drift spaces made by ion implantation," *Proc. IEEE* (Lett.), vol. 58, pp. 1135–1136, July 1970.

[16] T. E. Seidel, R. E. Davis, and D. E. Iglesias, "Double-drift-region ion-implanted millimeter-wave IMPATT diodes," *Proc. IEEE*, vol. 59, pp. 1222–1228, Aug. 1971.

[17] H. J. Kuno, "Analysis of nonlinear characteristics and transient response of IMPATT amplifiers," this issue, pp. 694–702.